

# Rheological fluid motion in tube by metachronal waves of cilia

S. Maiti<sup>1,2</sup>\*, S. K. Pandey<sup>1</sup> †

<sup>1</sup>*Department of Mathematical Sciences  
Indian Institute of Technology (BHU),  
Varanasi-221005, India*

<sup>2</sup> Department of Mathematics, The LNM Institute of Information Technology  
Jaipur 302031, India

## Abstract

This paper presents a theoretical study of a non-linear rheological fluid transport in an axisymmetric tube by cilia. However, an attempt has been made to explain the role of cilia motion on the transport of fluid through the ductus efferentes of the male reproductive tract. Ostwald-de Waele power-law viscous fluid has been considered to represent the rheological fluid. To analyze pumping by means of a sequence of beat of cilia from row-to-row of cilia in a given row of cells and from one row of cells to the next (metachronal wave movement), we consider the conditions that the corresponding Reynolds number is small enough for inertial effects to be negligible and the wavelength to diameter ratio is large enough for the pressure to be considered uniform over the cross-section. Analyses and computations of the detailed fluid motion reveal that the time-averaged flow rate is dependent on  $\epsilon$ , a non-dimensional measure involving the mean radius  $a$  of the tube and the cilia length. Thus, flow rate significantly varies with the cilia length. Moreover, the flow rate has been reported near to the estimated value  $6 \times 10^{-3} ml/h$  for human efferent ducts if  $\epsilon$  is near by 0.4. The estimated value was suggested by Lardner and Shack [1] in human, based on the experimental observations for flow rates in efferent ducts of other animals, e.g., rat, ram and bull. In addition, the nature of the rheological fluid, i.e., the value of the fluid index  $n$  strongly influences various flow-governed characteristics. The interesting feature of the paper is that the pumping improves with the thickening behavior

---

\*Corresponding author, Email address: [maiti000000somnath@gmail.com](mailto:maiti000000somnath@gmail.com)/[somnath.maiti@lnmiit.ac.in](mailto:somnath.maiti@lnmiit.ac.in) (*S. Maiti*)

†Email address: [skpandey.apm@itbhu.ac.in](mailto:skpandey.apm@itbhu.ac.in) (*S. K. Pandey*)

for small values of  $\epsilon$  or in free pumping ( $\Delta P = 0$ ) and pumping ( $\Delta P > 0$ ) regions.

*Keywords: Non-Newtonian Fluid; Cilia Movement; Metachronal Wave; Volumetric Flow, Flow Reversal; Velocity at Wave Crest and Trough.*

*Chinese Library Classification: O357.2, O361.3 2010*

*Mathematics Subject Classification: 76A05, 76W05, Q66*

## 1 Introduction

The ductus efferentes are a series of microvessels which provide vital link between the testis and the epididymis [2]. It is known that the wall structure of these vessels is as a single layer of columnar epithelium which is supported by a thin layer of smooth muscle and connective tissue [3]. The function of the vessels are sperm transport from the rete testis to the epididymis and reabsorbing high amount of fluid which coming from the rete testis. Due to the second function, spermatozoa concentration raises to multifold. Epithelium of the ductus efferentes is composed by ciliated and non-ciliated cells. The well-formed tufts of cilia are projected by the ciliated cells from the lumen of the duct and closely-packed, long and regular microvilli are born by the non-ciliated cells. However, microvilli, which are scattered between the cilia, are also projected by the ciliated cells; but they are fewer, shorter and thinner than those of the non-ciliated cells. Since ductus efferentes are lined by ciliated epithelium, they are unique of the male reproductive tract [2, 3].

A cilium is a hairlike slender appendage/protuberance that projects from the free surfaces of certain cells (e.g. eukaryotic cells). Its presence has been observed in almost all animals. Due to their motility, it engages a significant role in various physiological processes like locomotion, alimentation, circulation, respiration and reproduction [1].

Cilia are classified into motile and non-motile cilia. The latter is also known as primary cilia. In this study, we have considered motile cilia which do not beat randomly; but rather in coordinated manner. This nature of the cilia possesses some important aspects of ciliated epithelium. A good deal of general observations and inferences on the cilia of the gill of several aquatic species were presented by Rivera [4] as: (a) In any given tissue, beat rate of all the cilia is quite uniform. (b) The lashings of a single cilium and of cilia on adjacent cells are very much coordinated. (c) A definite metachronal rhythm is established. Metachronal rhythm is a movement consisting of a sequence of beat from row to row of cilia in a given row of cells and then from one row of cells to the next one. As a result, any object, which is at rest on the

surface of cilia, always moves forwards keeping the direction fixed.

Since metachronal rhythm gives more fixed passage of water with time over the surface of cilia or perhaps it is impractical to stimulate synchronous beat of large area (Sleigh [5, 6]), it is believed that cilia beat in a metachronal rhythm to the contrary of synchronous manner. However, the metachronal rhythm along the surface of cilia may alter their pattern (Sleigh [5]). The change depends on whether the metachronal rhythms move towards the effective stroke of the ciliary beat (symplectic metachronism), or the metachronal rhythms pass towards the opposite of the effective stroke of the beat and so in the reverse direction of flow (antiplectic metachronism), or the cilia beat at right angles to the line of wave movement (diaplectic metachronism). Satir [51] presented a diaplectic meachronal rhythm as an example in Figure 6 in his study. There are some data available for some other animals as wave-lengths, metachronal rhythm velocities and frequencies (Sleigh [5]).

It is a bit debatable as to what extent the cilia and to what extent smooth muscles drive the fluid in the efferent ducts of the male reproductive tract. It was reported that the prime contribution of the net fluid transport in efferent ducts was coming from metachronal movement of cilia (cf. Lucas [7], Setchell [8]). However, Winet [9] created a cilio peristaltic model which suggested that the greater contribution to the flow was coming from the smooth muscle contraction. Winet [9] remarked that “we may conclude that if the peristaltic wave has a 33% or more constriction, the spermatozoa concentration in the ductus efferentes is at least  $4 \times 10^8$  cells  $cm^{-3}$  and that flow rates in the ductus efferentes are the same as in the rete testis”. However, he added that “no observations of  $\phi$  (the occlusion factor) have been made for any of the male tubes”. Epithelium of ductus efferentes is supported by only a thin layer of smooth muscle and connective tissue ([3], Page No. 439, 3rd paragraph). So the suggestion, the major contribution to the flow was from smooth muscle contraction, is questionable. Moreover, if the peristaltic wave has a 50% or more constriction and cilia length is more than  $20\mu m$ , cilia of opposite boundary will clash with each other at the contraction region. In addition, at the contraction region, the driving force (which is opposite direction of the flow) at the central region will be active on the cilia (which obstruct the free space at the central portion). As a result, there may be damage of cilia indicating that smooth muscle contraction (i.e. peristaltic motion) may not be the main driving force of fluid transport at ductus efferentes. Conclusion of this paper will throw some more light on this issue.

Ilio and Hess [3] stated that the ratio of ciliated and non-ciliated cells in the epithelium in different animals generally varies in range between 1:3 and 1:8 (cf. Benoit [10]). So the vast

majority of the inner surface is non-ciliated. However, Aire and Josling [11] reported (based on their experimental observations) that the cilia of the ciliated cells usually over-shadowed the luminal surfaces of non-ciliated cells even though the non-ciliated cells are greater than the ciliated cells in number (cf. Aire and Josling, pages 194-196, Fig. 9-15). Moreover, in histological photographs (cf. Aire and Josling [11], Fig. 12, Page No. 195), it is clear that ciliated and non-ciliated cells are not distinctly separated into two parts; they are rather adequately mixed to justify the model considered here.

It is to be noted that data are not easily obtainable for bigger animal species, especially mammals. However, it was measured that the beat frequency for cilia lining in the rabbit oviduct was approximately 20-30 beats/sec (Borell et al. [12]). It is worth mentioning that we can compare this order of magnitude of the frequency of cilia beat to the lower animals (Sleigh [5]).

It is to be further noted that several investigators (c.f. Jahn and Bovee [13, 14] and the references therein) studied the hydrodynamics of protozoa which utilize cilia for locomotion. Blake [15, 16] took a spherical envelope model in order to study the swimming of the protozoan opalina and the swimming motion considering the ciliated body either a two-dimensional or cylindrical shape. Miller [17, 18, 19] investigated mucus transport with the help of mechanical simulation of the cilia in the trachea, while Barton and Raynor [20] studied mucus transport analytically in the trachea without considering the metachronal rhythm. Those investigations on protozoology and mucus transport in the respiratory tract gave conception in terms of locomotion in protozoa as well as movement of particles in the respiratory tract. However, only a little has been done finding the relation between the properties of the cilia and the nature of the metachronal rhythm for fluid movement in efferent ducts. Our motivation came up from the questions related to the interpretation of the fluid movement through the ductuli efferentes of male reproductive tract of human (Greep [21]) and the effect of cilia on ovum transport and sperm movement in fallopian tubes (Blandau [22]), (Sturgis [23]). Particularly, this paper will deal with a comparison of the results for the flow rate of this model to the corresponding estimated flow rate in the ductuli efferentes of male reproductive tract.

It is worth to mention that there are limited data available on the flow rate due to ciliary activity. Based on the experimental observations (Setchell [8], Tuck et al. [24], Waites and Setchell [25]), Lardner and Shack [1] estimated flow rate for human testes as  $6 \times 10^{-3} ml/hr$  with approximate values, i.e.,  $a = 50 \mu m$  and frequency of beat of the cilia as 20/sec. But the theoretical model of Lardner and Shack [1] obtained a flow rate of  $0.12 \times 10^{-3} ml/hr$ . Hence,

further investigations are indeed required.

Past experimental observations indicate that most of the biological fluids possess non-Newtonian behaviour [26, 27, 28, 29, 30, 31, 32, 33, 34, 35, 36, 37]. Analyses on the basis of simple Newtonian fluid yield non realistic results. The power law model is one of the widely used model for rheological fluid transport [30, 31, 32, 33, 38, 39, 40]. The rheological nature of this model is strongly dependent on the rheological fluid index  $n$ . The model approximates both shear-thinning ( $n < 1$ ) and shear-thickening ( $n > 1$ ) fluids behaviour over a large range of rheological conditions [26, 27, 30, 31]. Viscous properties of human semen is experimentally found to exhibit power law-behaviour (Dunn and Picologlu [27], Mendeluk et al. [28]). It has been reported experimentally that semen proves to fit in a power-law model with pseudoplastic behavior [27, 28]. Thus studies on fluid transport of the power law model by ciliary activity is expected to yield some important inferences. Constitutive equation of a Newtonian fluid (i.e., relationship between shear stress and strain rate) is linear, whereas it is nonlinear for a rheological power-law fluid.

There are two different approaches for investing the periodic motion of cilia—the sub-layer model and the envelope model [41]. Sub-layer model approach helps us by computing the forces and bending moments generated by each cilium to neighbouring liquid and it obtains the mean flow generated above the cilia layer. But the hydrodynamic representation is wearisome and normally obtained numerically [15, 42, 43, 44]. The envelope model approach has advantage for the consideration of metachronal rhythms above the cilia layer ignoring the details of the sub-layer dynamics. Moreover, the envelope model can be utilized for comparing, even quantitatively, e.g., for comparing the swimming velocities evaluated mathematically with those reported in water for a number of microorganisms [16, 44, 45]. In addition, this approach is accountable to perturbation analysis and has been used to combine some non-Newtonian effects by a systematic way [44, 46, 47].

Recently, Siddiqui et al. [48] have studied the flow of a power law fluid due to ciliary motion in an infinite channel. They pointed out that the power-law fluid gives results closer to the estimated one as  $6 \times 10^{-3} ml/hr$ . However, we believe that in real physiology, the wall contraction/length related to cilia and favourable pressure gradient less than that they have considered. They took  $\epsilon = 0.9$ , giving reference to Agarwal and Anawaruddin [49] who had reported an application of their model for fluid transport in vas deferens. It is worth mentioning that ductus efferentes and vas deferens are quite different ducts, the latter one may undergo possibly that much wall contraction.  $\epsilon$ , a non-dimensional measure with respect to mean radius

$a$  of the tube and the cilia length, would be much less than  $\epsilon = 0.9$  [1, 50]. To the authors' knowledge, the other unacceptable considerations in [48] are: (i) they considered a large constant favourable pressure gradient. (ii) dependence of flow characteristics on higher value of  $\delta$ , wave number of the metachronal wave.

It is well known that pressure gradient in small biological vessels (at least when there is a wave like peristaltic wave [5, 31, 51, 52, 53], metachronal wave etc in the vessels) varies with the length of the vessels and favourable pressure gradients are physiologically insignificant, in general, and, at least, in the ductus efferentes ([9]). Moreover, study of flow characteristics is not true for higher values of  $\delta$  as they have done analysis for small values of  $\delta$ . However, their power law model is somehow different form and complex than compared with widely used power-law model.

In view of all the above, a theoretical model is being considered for more realistic consequences for the flow in an axisymmetric tube under the influence of metachronal rhythm of cilia movement. We study here a non-linear problem of Ostwald-de Waele power-law fluid transport induced by means of a sequence of cilia beat from row-to-row of cilia in a given row of cells and from one row of cells to the next (metachronal wave movement). The conditions considered in this study are small Reynolds number and small wave number.

Based upon the analytical investigation, the velocity, pressure difference, flow rate have been calculated. Thereafter, we have carried out extensive numerical calculations. Keeping in view a specific situation of fluid movement in micro-vessels by ciliary motion, the numerical results are exhibited in graphs. The results discussed for shear thinning and shear-thickening fluids are closely connected in the circumstances of various situations of fluid transport due to ciliary activity. For example, semen behaviour is normally of shear-thinning kind when it contains a number of spermatozoa up to certain limit; however, in the case of heavily concentrated spermatozoa suspensions, the nature of semen may be considered as shear-thickening type [27, 28, 29]. Moulik et al. [54] reported that high viscosity of semen might indicate antibodies in the plasma and/or genital tract infection.

Some novel features are discussed to have a better insight of fluid motion by ciliary activity. We can utilize ciliary pumping mechanism in the study of the hydrodynamics of protozoa which use cilia for locomotion. The results may find useful applications in cilia-based actuators as micro-mixers for flow control in tiny bio-sensors and also as micro-pumps for drug-delivery systems.

In this investigation, the term cilia will not consider flagella but ciliated epithelium. Com-

parative physiology of flagella including sperm tails may be available in [5, 55].

## 2 Formulation

A non-linear problem, concerning the fluid movement characteristics in an axisymmetric tube under the action of ciliary beat that generate a metachronal rhythm, is to be studied here by considering the fluid as an incompressible non-Newtonian viscous fluid. We consider an axisymmetric tube with ciliated walls of large length compared with its radius and a symplectic metachronal wave is moving in the righthand side having velocity  $c$ . The non-Newtonian viscous fluid behaviour within the tube is considered to be incompressible Ostwald-de Waele power law rheological fluid.

We treat  $(R, \theta, Z)$  as the cylindrical co-ordinates for the position of any fluid particle. Here,  $R$  is measured along the radius of the tube, the coordinate  $Z$  is along the wave propagation direction and  $\theta$  being the rotational coordinate. When  $\tau$ ,  $\Delta$  denote the stress tensor, symmetric rate of deformation tensor respectively, the governing law of shear stress for the Ostwald-de Waele power law fluid may be written as [56]

$$\tau = -\gamma \left\{ \left| \sqrt{\frac{1}{2}(\Delta : \Delta)} \right|^{n-1} \right\} \Delta, \quad (1)$$

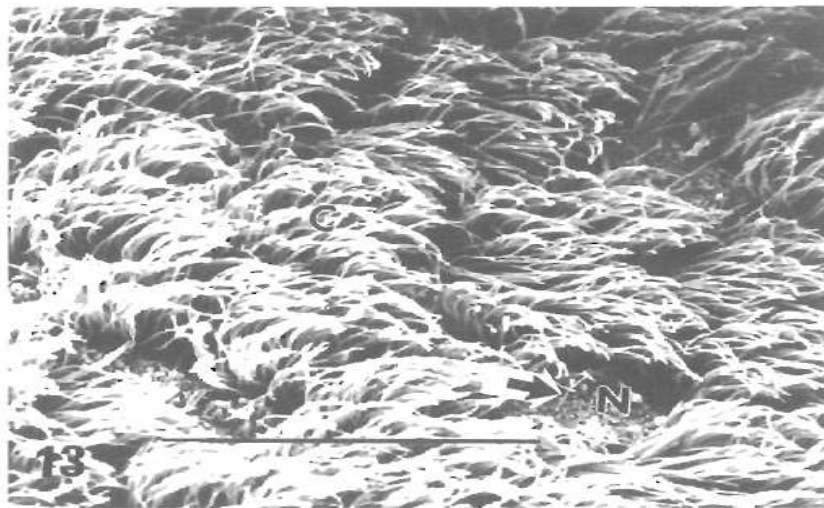
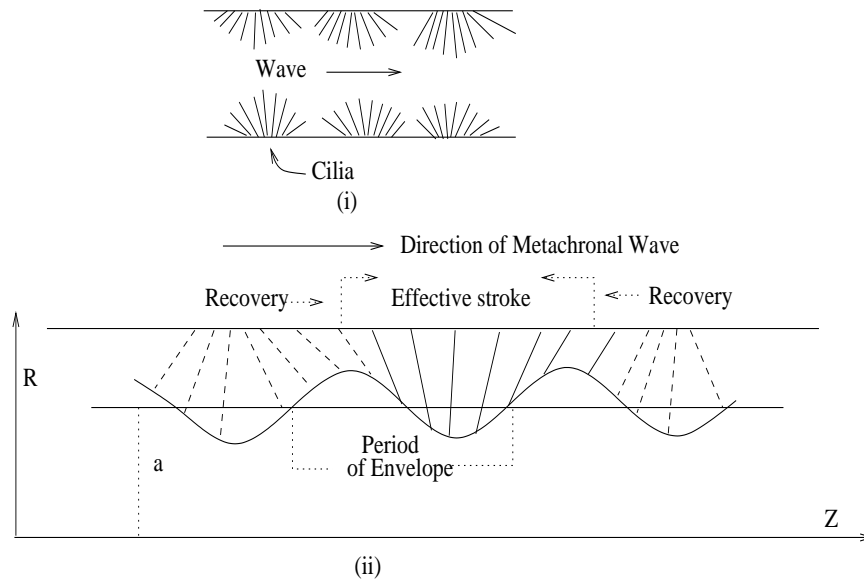
$$\text{where } \frac{1}{2}(\Delta : \Delta) = 2 \left( \left( \frac{\partial V}{\partial R} \right)^2 + \left( \frac{V}{R} \right)^2 + \left( \frac{\partial U}{\partial Z} \right)^2 \right) + \left( \frac{\partial U}{\partial R} + \frac{\partial V}{\partial R} \right)^2,$$

where  $\gamma$ ,  $n$  are respectively the flow consistency index and power-law index respectively. We introduce  $U$  and  $V$  as the velocity components respectively in the  $Z$ ,  $R$  directions. We know that shear thinning fluid has been classified for  $n < 1$  and  $n > 1$  corresponds to shear thickening fluid.

Under the above consideration, the flow of an incompressible viscous Ostwald-de Waele power-law fluid in an axisymmetric tube together with equation of continuity may be considered to be governed by

$$\frac{1}{R} \frac{\partial(RV)}{\partial R} + \frac{\partial U}{\partial Z} = 0, \quad (2)$$

$$\rho \left( \frac{\partial U}{\partial t} + U \frac{\partial U}{\partial Z} + V \frac{\partial U}{\partial R} \right) = -\frac{\partial P}{\partial Z} - \frac{1}{R} \frac{\partial(R\tau_{RZ})}{\partial R} - \frac{\partial \tau_{ZZ}}{\partial Z}, \quad (3)$$



(This Fig. taken from Ref. [43])

(iii)

Figure 1: Wave motion of Cilia: (i) Ciliated tubule, (ii) metachronal wave pattern (iii) a SEM micrograph of the luminal surface of the distal efferent duct (DED) of the turkey, showing ciliated (C) , and non-ciliated (N) cells. Arrow, single cilium of a non-ciliated cell. Bar =  $20\mu m$ . Perfusion fixation (cf. Ref. [11])



$$\rho \left( \frac{\partial V}{\partial t} + U \frac{\partial V}{\partial Z} + V \frac{\partial V}{\partial R} \right) = -\frac{\partial P}{\partial R} - \frac{1}{R} \frac{\partial (R\tau_{RR})}{\partial R} - \frac{\partial \tau_{RZ}}{\partial Z}, \quad (4)$$

where  $\rho$  and  $P$  are the density and pressure of the fluid respectively. Geometry of the metachronal wave pattern helps us to assume the envelope of the cilia tips mathematically by

$$R = H = f(Z, t) = a + a\epsilon \cos \left( \frac{2\pi}{\lambda} (Z - ct) \right). \quad (5)$$

This can be therefore assumed as the equation of the extensible vessel wall. Here ‘ $a$ ’ is mean radius of the tube and  $\epsilon$  be a non-dimensional parameter which together with ‘ $a$ ’ in the form of ‘ $a\epsilon$ ’ makes the amplitude of the metachronal wave.  $\lambda$ ,  $c$  are the metachronal wave length and velocity respectively. Observations of the various patterns of cilia movement in [6] motivate us to assume the cilia tips to move in elliptical paths so that the horizontal position of a cilia tip is in an implicit form

$$Z = g(Z, Z_0, t) = Z_0 + a\epsilon\alpha \sin \left( \frac{2\pi}{\lambda} (Z - ct) \right), \quad (6)$$

in which  $Z_0$  represents a reference location of the particle,  $\alpha$  stands for a measure of the eccentricity of the elliptical motion. Under the no slip condition, the velocities imparted to fluid particles are just those of the cilia tips. Thus, the axial and vertical velocities of the cilia are evaluated as

$$U = \frac{\partial Z}{\partial t} \Big|_{z_0} = \frac{\partial g}{\partial t} + \frac{\partial g}{\partial Z} \frac{\partial Z}{\partial t} = \frac{\partial g}{\partial t} + \frac{\partial g}{\partial Z} U, \quad (7)$$

$$V = \frac{\partial R}{\partial t} \Big|_{z_0} = \frac{\partial f}{\partial t} + \frac{\partial f}{\partial Z} \frac{\partial Z}{\partial t} = \frac{\partial f}{\partial t} + \frac{\partial f}{\partial Z} U. \quad (8)$$

If the equations (5) and (6) are applied to the equations (7) and (8), we obtain

$$U = \frac{\frac{-2\pi a c \alpha \epsilon}{\lambda} \cos \left( \frac{2\pi}{\lambda} (Z - ct) \right)}{1 - \frac{2\pi a \alpha \epsilon}{\lambda} \cos \left( \frac{2\pi}{\lambda} (Z - ct) \right)} \quad (9)$$

$$V = \frac{\frac{2\pi a c \epsilon}{\lambda} \sin \left( \frac{2\pi}{\lambda} (Z - ct) \right)}{1 - \frac{2\pi a \alpha \epsilon}{\lambda} \cos \left( \frac{2\pi}{\lambda} (Z - ct) \right)} \quad (10)$$

These boundary conditions enable us to distinguish between the effective stroke of the cilia and the slow less effective recovery stroke by approximately accounting for the shortening of the cilia. Hence, the tube is narrower when  $U$  is positive at the boundary.

For a wave frame  $(z, r)$  moving with a velocity  $c$  away from a fixed frame  $(Z, R)$ , let us apply the transformations

$$z = Z - ct, \quad r = R, \quad u = U - c, \quad v = V, \quad p(z, t) = P(Z, R, t), \quad (11)$$

where  $(u,v)$ ,  $(U,V)$  denote the velocity components,  $p$  and  $P$  are respectively pressure in wave frame and fixed frame of reference. Afterward, we will introduce the following non-dimensional variables:

$$\begin{aligned}\bar{z} &= \frac{z}{\lambda}, \quad \bar{r} = \frac{r}{a}, \quad \bar{u} = \frac{u}{c}, \quad \bar{v} = \frac{v}{c\delta}, \quad \delta = \frac{a}{\lambda}, \quad \bar{p} = \frac{a^{n+1}p}{\gamma c^n \lambda}, \quad \bar{t} = \frac{ct}{\lambda}, \quad h = \frac{H}{a}, \\ Re &= \frac{\rho a^n}{\gamma c^{n-2}} \frac{a}{\lambda}, \quad \bar{\tau}_{rz} = \frac{\tau_{rz}}{\gamma \left(\frac{c}{a}\right)^n}, \quad \bar{Q}_1 = \frac{Q_1}{\pi a^2 c},\end{aligned}\quad (12)$$

where  $Q_1(Z, t)$  is the instantaneous volume flow rate and  $Re$  is Reynolds number of the fluid flow. Dropping the bars over the symbols, the equations governing the flow can be rewritten as

$$\frac{1}{r} \frac{\partial(rv)}{\partial r} + \frac{\partial u}{\partial z} = 0, \quad (13)$$

$$Re \left( \frac{\partial u}{\partial t} + u \frac{\partial u}{\partial z} + v \frac{\partial u}{\partial r} \right) = -\frac{\partial p}{\partial z} + \frac{1}{r} \frac{\partial}{\partial r} \left( \Phi \left( r \frac{\partial u}{\partial r} + r \delta^2 \frac{\partial v}{\partial z} \right) \right) + 2\delta^2 \frac{\partial}{\partial z} \left( \Phi \frac{\partial u}{\partial z} \right), \quad (14)$$

$$Re\delta^2 \left( \frac{\partial v}{\partial t} + v \frac{\partial v}{\partial z} + v \frac{\partial v}{\partial r} \right) = -\frac{\partial p}{\partial r} + \delta^2 \frac{1}{r} \frac{\partial}{\partial r} \left( r \Phi \frac{\partial v}{\partial r} \right) + \delta^2 \frac{\partial}{\partial z} \left( \Phi \left( \frac{\partial u}{\partial r} + \delta^2 \frac{\partial v}{\partial z} \right) \right), \quad (15)$$

$$\Phi = \left| \sqrt{2\delta^2 \left\{ \left( \frac{\partial v}{\partial r} \right)^2 + \left( \frac{v}{r} \right)^2 + \left( \frac{\partial u}{\partial z} \right)^2 \right\} + \left( \frac{\partial u}{\partial r} + \delta^2 \frac{\partial v}{\partial z} \right)^2} \right|^{n-1}; \quad (16)$$

whereas the boundary conditions are

$$\frac{\partial u}{\partial r} = 0 \text{ at } r = 0 \text{ and } u = \frac{-2\pi\alpha\delta\epsilon \cos(2\pi z)}{1 - 2\pi\alpha\delta\epsilon \cos(2\pi z)} - 1, \quad (17)$$

$$v = \frac{2\pi\epsilon \sin(2\pi z)}{1 - 2\pi\alpha\delta\epsilon \cos(2\pi z)}, \quad (18)$$

on  $r = h = 1 + \epsilon \cos(2\pi z)$ .

Since in most of the cases of flow in small diameter tubules, Reynolds numbers are very small ( $Re \ll 1$ ), the analysis can be carried out by the approximation of the inertia-free flow. Moreover, in the wave frame of reference, if the tube length is finite and equal to an integral number of wavelengths together with constant pressure difference across the ends of the tube, the flow may be steady [53]. In this case, the governing equations under the consideration of the long-wavelength approximation (which makes  $\delta \ll 1$ ) can be simplified as follows:

$$0 = -\frac{\partial p}{\partial z} + \frac{1}{r} \frac{\partial}{\partial r} \left( r \frac{\partial u}{\partial r} \left| \frac{\partial u}{\partial r} \right|^{n-1} \right) \quad (19)$$

$$0 = -\frac{\partial p}{\partial r} \quad (20)$$

and also the simplified forms of the boundary conditions may be given by

$$\frac{\partial u}{\partial r} = 0 \text{ at } r = 0 \text{ and } u = u(h) = -1 - 2\pi\alpha\delta\epsilon \cos(2\pi z), \quad (21)$$

$$v = v(h) = 2\pi\epsilon \sin(2\pi z) + 2\pi^2\epsilon^2\alpha\delta \sin(4\pi z), \quad (22)$$

on  $r = h = 1 + \epsilon \cos(2\pi z)$ . By solving (19) subject to the boundary conditions (21), we find the axial velocity in the form

$$u(r, z) = u(h) + \frac{p_1|p_1|^{k-1}}{2^k(k+1)} [r^{k+1} - h^{k+1}], \quad (23)$$

where  $p_1 = \frac{\partial p}{\partial z}$  and  $k = \frac{1}{n}$ . If we integrate the continuity (13) across the cross section of the tube, we get

$$2 \int_0^h \frac{1}{r} \frac{\partial(rv)}{\partial r} r dr + 2 \int_0^h \frac{\partial u}{\partial z} r dr = 0 \quad (24)$$

$$\text{or, } rv|_h - rv|_0 + \frac{\partial}{\partial z} \int_0^h ur dr - hu(h, z, t) \frac{\partial h}{\partial z} - 0 \times u(0, z, t) = 0 \quad (25)$$

$$\text{or, } hv(h) + \frac{1}{2} \frac{\partial q}{\partial z} - h \frac{\partial h}{\partial z} u(h) = 0, \text{ where } q = 2 \int_0^h ur dr \quad (26)$$

which implies that  $\frac{\partial q}{\partial z} = 2h \left( \frac{\partial h}{\partial z} u(h) - v(h) \right) = 0$ .

This shows the fixed volume flow rate  $q$  in the wave frame of reference. By integrating (23) across the cross section of the tube, pressure gradient is obtained in terms of the volume flow rate in the following form:

$$q = h^2 u(h) - \frac{p_1|p_1|^{k-1} h^{k+3}}{2^k(k+3)}. \quad (28)$$

Putting  $dp/dz$ , which obtained from (28), into (23) we calculate

$$u(r, z) = u(h) + \frac{(k+3)(q - h^2 u(h))}{(k+1)h^{k+3}} [h^{k+1} - r^{k+1}] \quad (29)$$

By integrating, the instantaneous non-dimensional volume flow rate,  $Q_1(Z, t)$ , in the fixed frame of reference, is found as

$$Q_1(Z, t) = 2 \int_0^h U(R, Z, t) R dR = q + h^2 \text{ (using the transformation formulae (11))} \quad (30)$$

Thus, the time-mean volume flow rate over a wave period is given by

$$Q(Z) = \frac{1}{T} \int_0^T Q_1(Z, t) dt = q + \frac{1}{T} \int_0^T h^2(Z, t) dt, \quad (31)$$

which, on integration for the sinusoidal wall of (5), gives

$$Q(Z) = q + 1 + \frac{\epsilon^2}{2} \quad (32)$$

Solving  $dp/dz$  from (28) and using (32), the pressure rise per wavelength may be given by the relation

$$\Delta p = \int_0^1 \frac{dp}{dz} dz = - \int_0^1 \left| \frac{2^k(k+3)(Q - 1 - \frac{\epsilon^2}{2} - h^2 u(h))}{h^{k+3}} \right|^{n-1} \left\{ \frac{2^k(k+3)(Q - 1 - \frac{\epsilon^2}{2} - h^2 u(h))}{h^{k+3}} \right\} dz. \quad (33)$$

It may be noted that if we set  $n = 1$ ,  $\alpha = 0$  in Equations (23), (28) and (33), the expressions reduce to those reported earlier in Ref. [53]. If  $\alpha = 0$ , the results also match well those of Ref. [30] when the peristaltic wave form in [30] is replaced by the metachronal wave in this study. Similarly, if the yield stress is set equal to zero and fluid flow is considered in an axisymmetric uniform vessel in [52], the expressions said above reduce to that obtained in [52].

By solving the continuity equation (13) subject to the boundary condition (22), we get the radial velocity as

$$v(r, z) = u(h) \frac{r^{k+2}}{h^{k+2}} \frac{\partial h}{\partial z} + \frac{h}{k+1} \left[ \frac{r}{h} - \frac{r^{k+2}}{h^{k+2}} \right] \frac{\partial u(h)}{\partial z} + \frac{(k+3)q}{(k+1)h^2} \left[ \frac{r}{h} - \frac{r^{k+2}}{h^{k+2}} \right] \frac{\partial h}{\partial z}. \quad (34)$$

### 3 Quantitative Study

This section deals with a quantitative study of the mathematical model considered in the above sections. It may be noted that unlike the Newtonian model, it has been not possible to find an explicit expression for pressure difference  $\Delta p$  in terms of time averaged flow rate  $Q$  for Ostwald-de Waele power law model. This is due to the complexity of the problem of a rheological fluid arising out of arbitrary wave shape. However, a numerical computation is required to express pumping characteristics or pumping performance of the rheological fluid for the sake of clarity. In addition, it is a convention to exhibit velocity field in term of pressure difference between the tube ends. Hence, in view of those observations and also in order to fulfill the requirements, necessary computations have been carried out numerically by using the software MATHEMATICA.

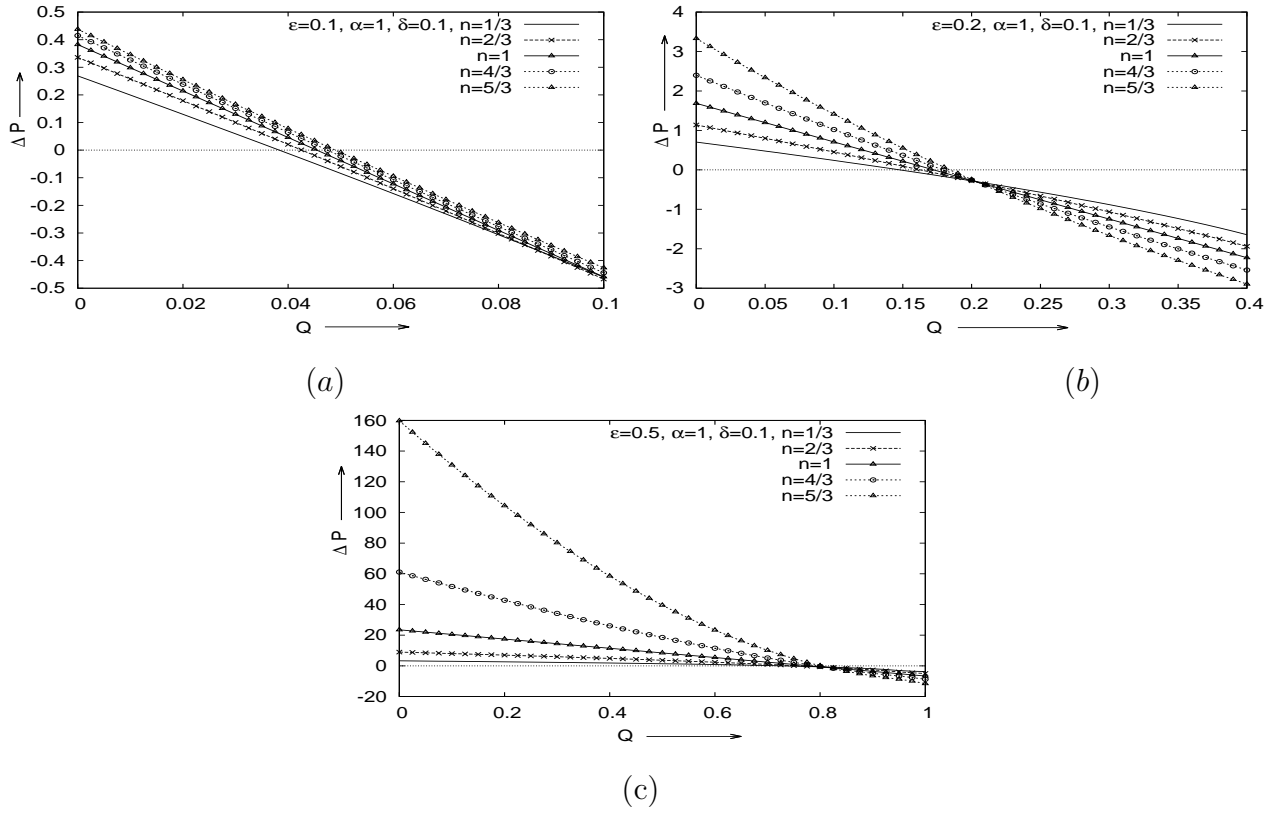


Figure 2: The diagrams exhibit the dependence of flow rate and pressure difference relation ( $Q - \Delta p$ ) on  $\epsilon$ , flow behaviour index  $n$  and eccentricity  $\alpha$ . In all the figures, wave number  $\delta = 0.1$ ,  $\alpha = 1$  and  $n$  has been varied from  $1/3$  to  $5/3$  to observe the changes taking place in  $Q - \Delta p$  relation. Effect of  $\epsilon$  on  $Q - \Delta p$  relation has been shown in Figs. (a-c) by varying  $\epsilon$  from 0.1-0.5.

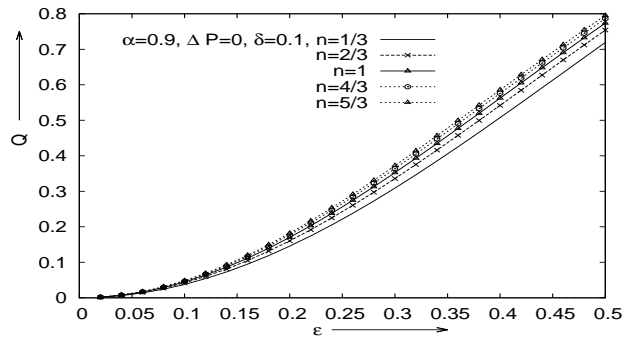


Figure 3: The diagram exhibits the dependence of flow rate  $Q$  and  $\epsilon$  relation on flow behaviour index  $n$  by plotting graphs for  $n=1/3-5/3$ . The other parameters are kept as  $\Delta p = 0$ , i.e. free pumping,  $\delta = 0.1$ ,  $\alpha = 0.9$ .

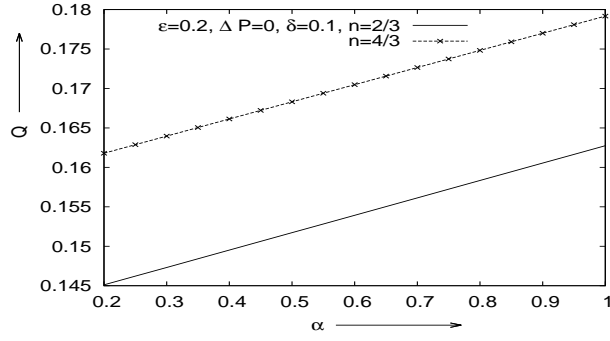


Figure 4: The diagram exhibits the dependence of flow rate  $Q$  and eccentricity  $\alpha$  relation on flow behaviour index  $n$  by plotting graphs for  $n=2/3-4/3$ . The other parameters are kept as  $\Delta p = 0$ , i.e. free pumping,  $\delta = 0.1$ ,  $\epsilon = 0.2$ .

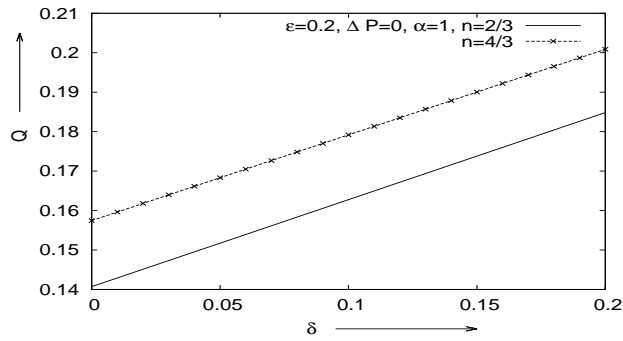


Figure 5: The diagram exhibits the relation of flow rate  $Q$  with wave number  $\delta$  and its dependence on flow behaviour index  $n$ , which has been shown by plotting graphs for  $n=2/3$  and  $4/3$ . The other parameters are kept as  $\Delta p = 0$ , i.e. free pumping,  $\alpha = 1$ ,  $\epsilon = 0.2$ .

It is to be noted that there are only a few available data on the flow rates due to ciliary activity [1, 50]. For the quantitative study, we shall present mathematical estimates of various physical quantities relevant to physical problems of the flows of rheological fluids under ciliary activity. For the present analysis, the following non-dimensional data for the rheological fluids have been used [1, 50]:

$$\epsilon = 0.1 \text{ to } 0.5, \alpha = 0.3 \text{ to } 1, \delta = 0.05 \text{ to } 0.2, n = \frac{1}{3} \text{ to } 2, Q = 0 \text{ to } 1.$$

### 3.1 Pumping Characteristics

It is natural to determine pressure-flow characteristic (i.e. the pumping characteristics) by the variation of time averaged flow rate  $Q$  with pressure difference  $\Delta P$  across one wave length. Variations of volumetric flow rate by cilia motion for different values of  $\epsilon$ , flow index number  $n$ , wave number  $\delta$  and eccentricity  $\alpha$  have been exhibited in Figs. 2-5. As expected, the variations are linear nature for an inertia-free flow ( $Re=0$ ) of a Newtonian fluid. The curves of  $\Delta P$  versus  $Q$  are straight lines with negative slope and positive intercepts; but, for the aforesaid case of a rheological fluid, the relation is nonlinear between the pressure difference and the mean flow rate.

The curves have three portions, namely, (i) free pumping zone, describing the region in which  $\Delta P = 0$ , (ii) pumping zone, indicating the region where  $\Delta P > 0$  and (iii) co-pumping zone, which is regarded for the region where  $\Delta P < 0$ , the situation favourable for the flow to take place. We can compute the amount of flow pumped by ciliary activity if the mean pressure gradient ( $\Delta P = 0$ ) is absent and also for the case of adverse pressure gradient (i.e  $\Delta P > 0$ ) up to a certain limit. If  $\epsilon$ ,  $n$ ,  $\delta$ ,  $\alpha$  are fixed at some values, employment of an adverse mean pressure gradient diminishes the mean flow rate obtained when  $\Delta P = 0$ ; and by the time it becomes right amount (certain limit), it is equal to the driving force of motion generated by the cilia movement, i.e. the mean flow reduces to 0. Further, if  $\Delta P (> 0)$  exceeds the limit, the fluid will move in the reverse direction.

Figs. 2(a-c) show that the area of the pumping zone and the length of the free pumping zone both increase significantly with a rise in  $\epsilon$  for Newtonian, shear thinning as well as shear thickening fluids. Also these (area, length) enhance at a very high rate with an increase in the rheological parameter  $n$ . In other words, for fixed values of  $\Delta P$ , time averaged flow rate  $\bar{Q}$  rises with an increase in  $\epsilon$  and  $n$ . However, in the co-pumping zone, there is a critical value of  $\Delta P$  for which  $Q$  can be raised for all fixed values of  $\Delta P$  with an increase in  $n$  when  $\epsilon$

$> 0.1$  . If  $\Delta P$  exceeds this critical value, the reverse trend occurs. It is important to mention that for fixed values of parameters, taken by Lardner and Shack together with  $n = 1$ , the flow rate in axisymmetric tube is twice the values reported by Lardner and Shack for a two-dimensional channel. In the case of free pumping, Fig. 3 clearly reveals that there is a remarkable enhancement of flow rate with increase in  $\epsilon$ . It further explains that  $n$  strongly influences the flow rate. The plots, presented in Figs. (4-5), indicate that for a non-Newtonian fluid,  $Q$  increase as the wave number  $\delta$  and  $\epsilon$  increase and these parameters enhance  $Q$  at almost the same rate for both the shear thinning and shear thickening fluids.

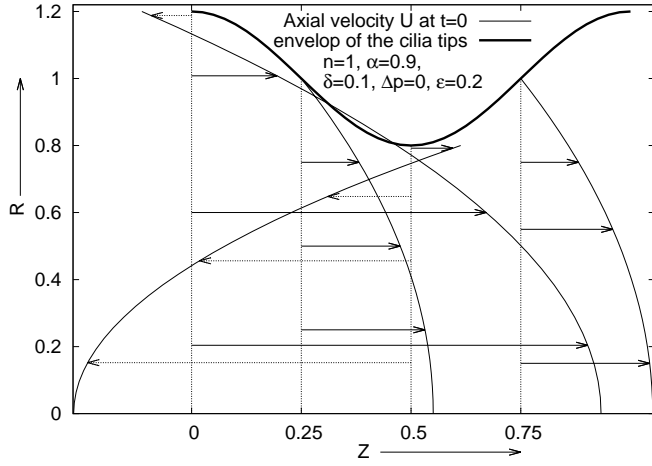
It is worthwhile to mention that an increase of  $\epsilon$  corresponds to rise of cilia length and vice versa. Again in the case of free pumping, when  $\epsilon=0$ , i.e., there are no cilia to the inner surface of the tube, then  $Q=0$ .

### 3.2 Distribution of Velocity

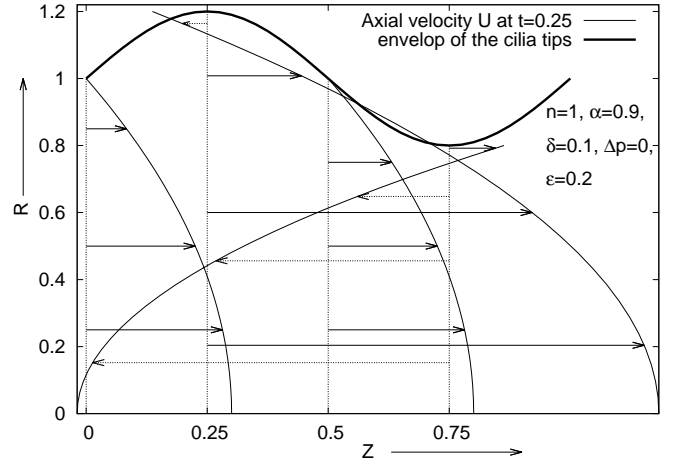
As shown in the previous section, the mean flow rate is only responsible to the flow through ciliary activity during free pumping and only the movement of cilia produces the driving force for fluid transport. For various values of  $\epsilon$ ,  $n$ ,  $\delta$  and  $\alpha$ , the distributions of axial velocity of the current investigation are presented in Figs. (6, 8-11). Since the flow is unsteady in the fixed frame of reference and the velocity profiles along with the lumen of the ductus efferentes vary with time, the distribution of velocity has been investigated at a time interval which is a quarter of a metachronal wave period of cilia.

One can observe from Fig. 6 that there exists a retrograde flow region at any time and the maximum retrograde flow occurs at the narrowest portion of the tube, while the maximum flow in the forward direction takes place at the the widest portion of the tube. As the time-averaged flow rate is positive for free-pumping (cf. Pumping Characteristic in the previous section), the forward flow region is predominant here. Moreover, the study further reveals the existence of two stagnation points on the axis. For example, at time  $t=0.75$ , one stagnation point lies between  $Z=0.0$ ,  $Z=0.25$  and the other is situated between  $Z=0.25$  and  $Z=0.5$  which separate the central region of a retrograde flow from two forward flow regions. Similar observations had been reported numerically and analytically by Takabatake and Ayukawa [57] and Maiti and Misra [33, 52], Misra and Maiti [31] for a Newtonian fluid and non-Newtonian fluids respectively for peristaltic transport. From the standpoint of ciliary pumping, this retrograde flow at the trough region is considered to be a kind of ineffective leakage.

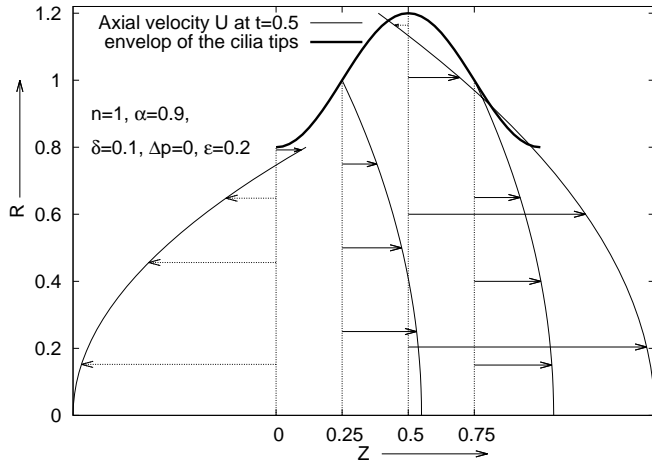




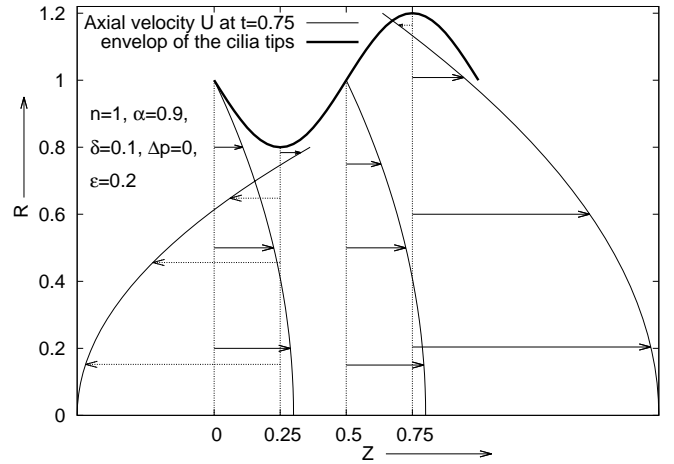
(a) Axial velocity at  $t=0$



(b) Axial velocity at  $t=0.25$



(c) Axial velocity at  $t=0.5$



(d) Axial velocity at  $t=0.75$

Figure 6: The dark coloured curves represent envelop of cilia tips in the diagrams. Within them and the central lines of the tubes are given axial positions, represented by vertical lines, of fluid particles considered at different instants of time ( $t = 0 - 0.75$ ) depicted in 4 different diagrams. The arrows emerging from the vertical lines indicate their velocities and directions which eventually form profiles indicated by curves touching the heads of the arrows. The arrows in the backward direction indicate retrograde flows.

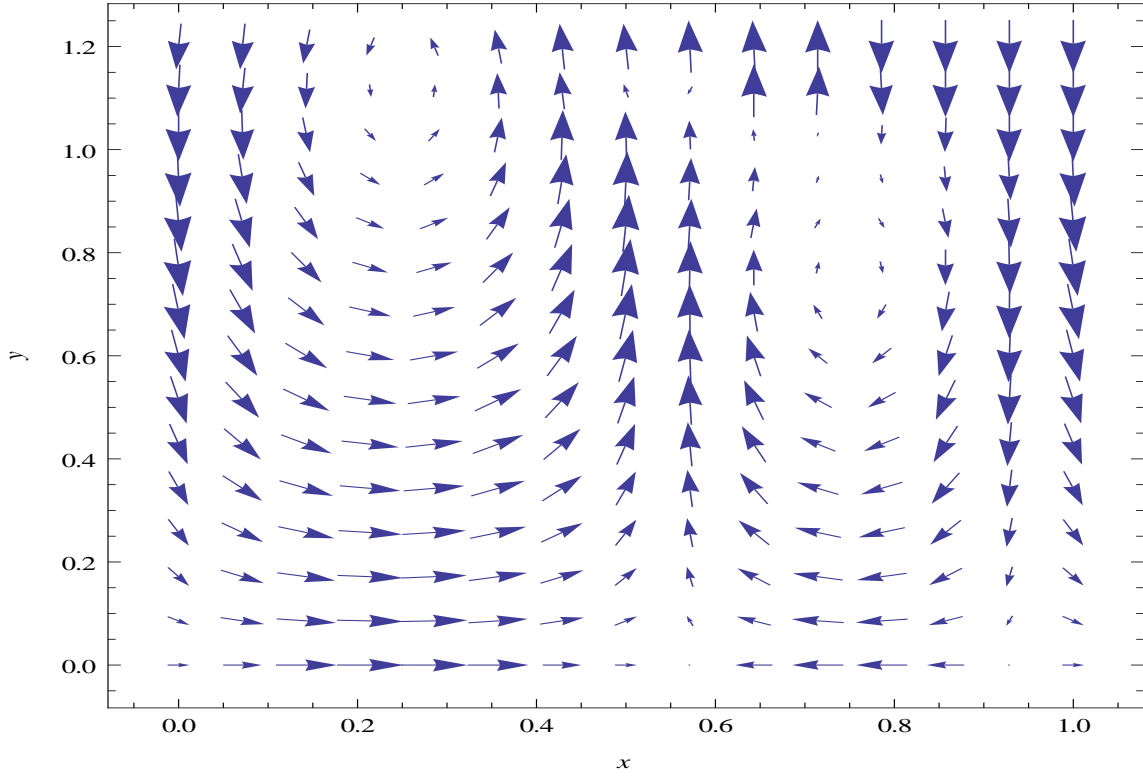
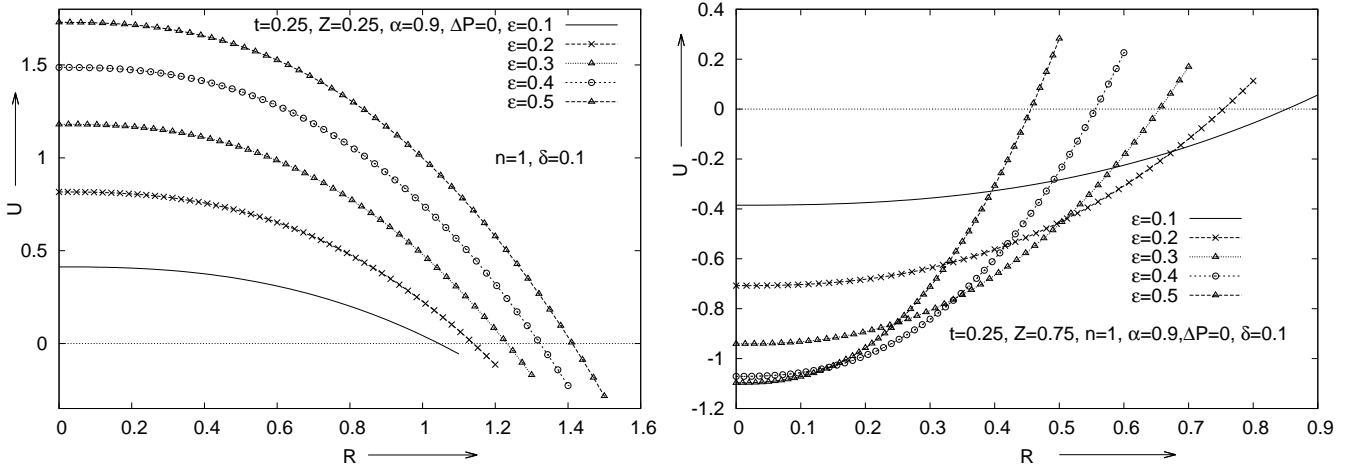


Figure 7: The diagram shows instantaneous flow field at time  $t=0.25$  of a Newtonian fluid ( $n = 1$ ) when  $\epsilon = 0.2$ ,  $\Delta P = 0$ ,  $\alpha = 0.9$ ,  $\delta = 0.1$ .



(a) Velocity distribution of Newtonian fluid at the wave crest

(b) Velocity distribution of Newtonian fluid at the wave trough

Figure 8: The diagrams show the distributions of velocities of a Newtonian fluid at the wave crest and the wave trough section for the different values of  $\epsilon$  when  $\Delta P = 0$ .

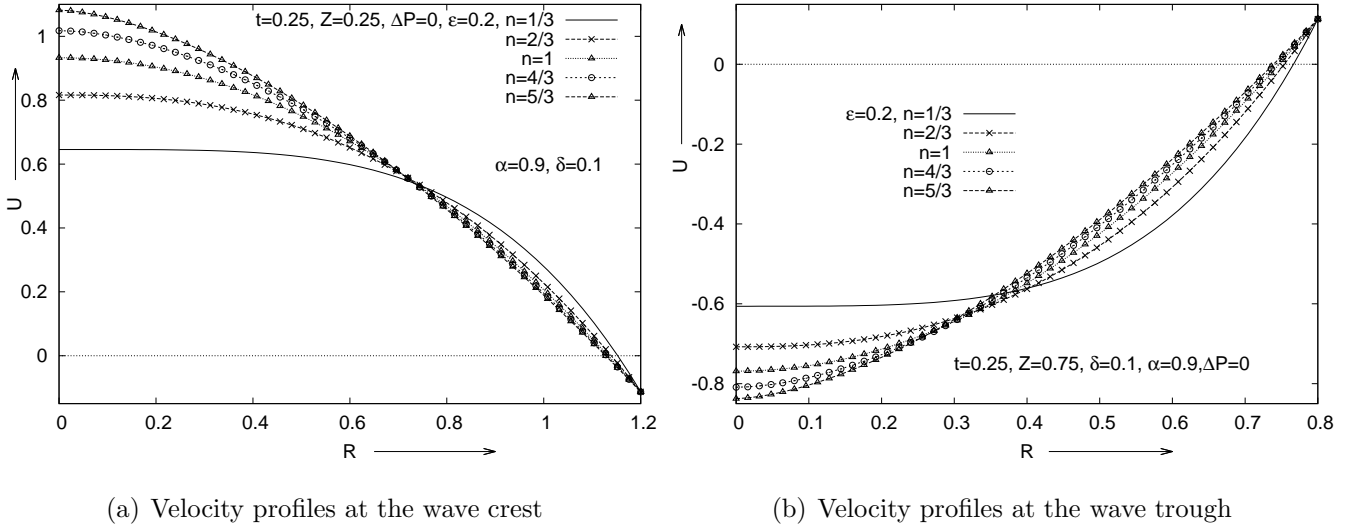
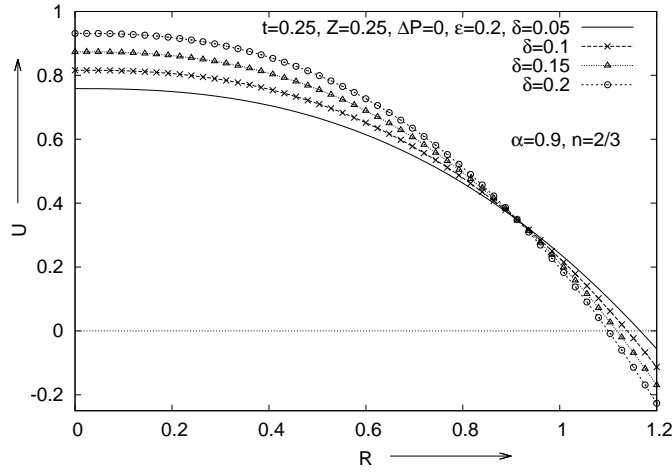


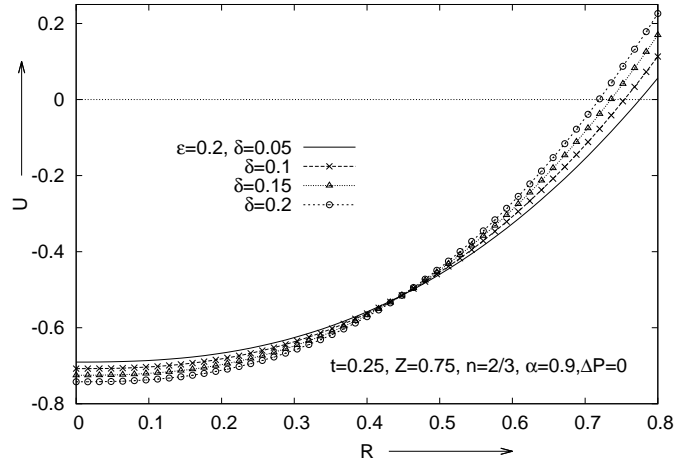
Figure 9: The diagrams exhibit the velocity profiles of the rheological fluids at the wave crest and the wave trough sections for the different values of flow behaviour index  $n$ .

It is to be noted that the beat of a single cilium have two different phases. One of them is the effective stroke of cilia, i.e., when the movement of cilium is in the general fluid movement direction. Reflux occurs near the walls in this case and the portion of the tube is wide. The other phase is the recovery stroke, i.e., when the movement of cilium is in the opposite direction to the general fluid movement. There may be forward flow near the walls and the narrow portion of the tube in this case. Fig. 7 shows instantaneous velocity field plot, the corresponding envelop of the cilia tips is shown in Fig. 6(b). The flow is along the direction of the cilia motion in the region  $0 \leq Z \leq 0.5$ , while the reverse trend occurs in the region  $0.5 \leq Z \leq 1$ .

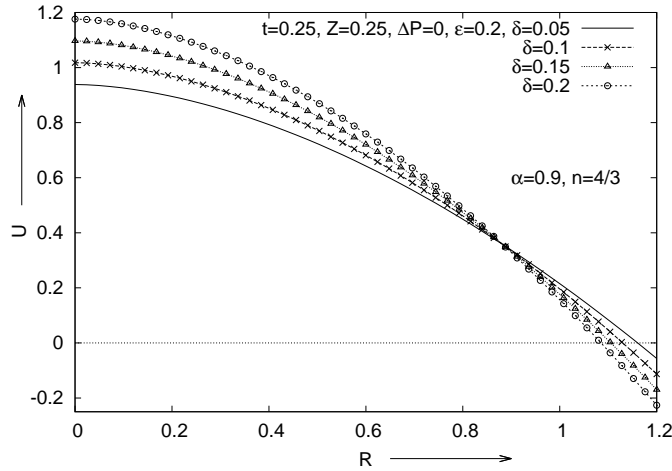
The effects of  $\epsilon$ ,  $n$ ,  $\delta$  and  $\alpha$  on the velocities at the crest and the trough section of the tube are shown in Figs. (8-11) under consideration of free-pumping. It may be observed from the Fig. (8) that there is a remarkable increase in the magnitude of the axial velocity due to an increase in the value of  $\epsilon$  for both sections. This may be interpreted that the rise of cilium length (at least up to a certain limit) may generate greater driving force. Fig. (9) illustrates that the magnitude of the axial velocity for both sections enhances significantly at the central region while the reverse trend occurs at the boundary region if flow index number  $n$  increases. That reverse trend might have been initiated due to the increase of  $n$  which in related to friction at the boundary region of the tube. As shown in Figs. (10-11), wave number  $\delta$  and eccentricity  $\alpha$  of the path of the cilia raise the magnitude of the axial velocity at the central region for both sections, while at the boundary region, the trend is reversed indicating enhancement of friction



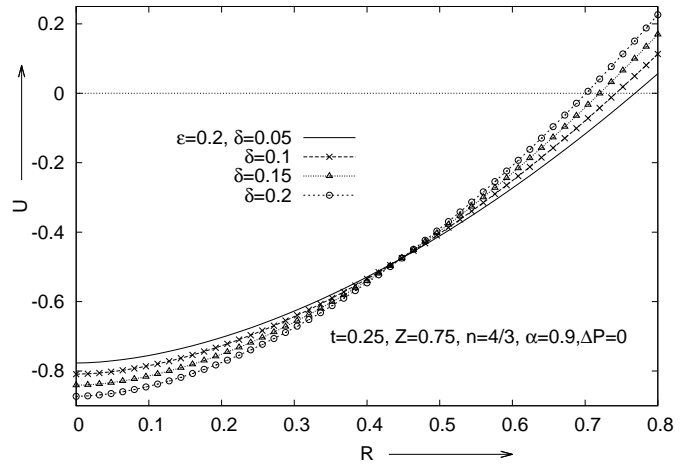
(a) Velocity profiles for a shear thinning fluid at the wave crest



(b) Velocity profiles for a shear thinning fluid at the wave trough



(c) Velocity profiles for a shear thickening fluid at the wave crest



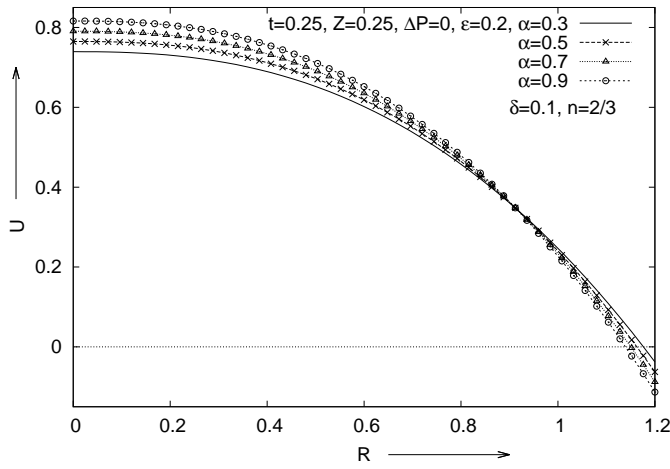
(d) Velocity profiles for a shear thickening fluid at the wave trough

Figure 10: The diagrams exhibit the velocity profiles of the rheological fluids at the wave crest and the wave trough sections for the different values of  $\delta$ .

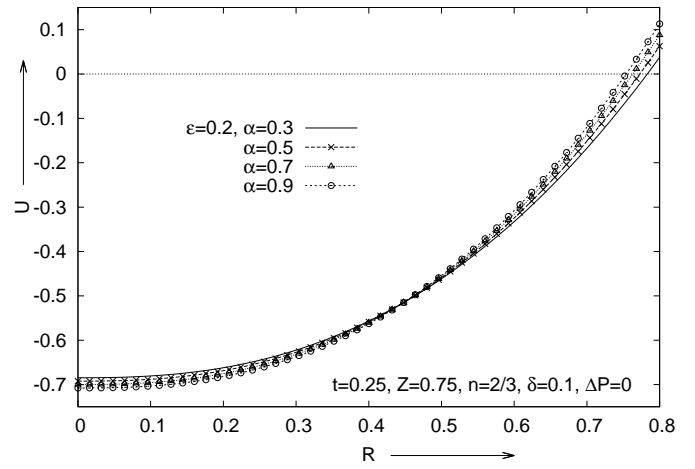
due to increase in  $\delta$  and  $\alpha$ .

## 4 Application to fluid movement in ductuli efferentes

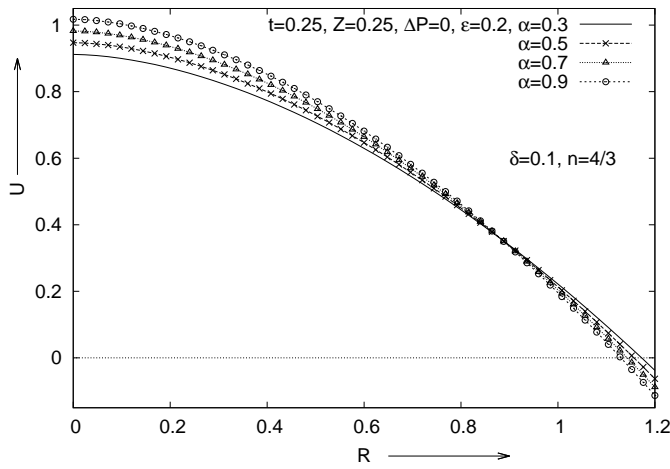
The ciliated walls of an axisymmetric tube have been modelled by metachronal wave of cilia which are equivalent to the wavy walls of peristaltic transport. There is only a few available data in the existing literature on the flow rates due to the ciliary activity. The relationship between the pressure difference and the time-mean-volume flow rate through an axisymmetric tube is given in (33). We have to verify whether the computations given by (33) reflect to the flow rates measured in efferent ducts of the male reproductive tract. In humans, the efferent ducts are 10-15 tubules connecting the rete testis to the epididymis and the lining cells in the tubules are ciliated. In general researchers believe that the cilia drive the fluid motion [21] through the efferent ducts. Lardner and Shack [1] estimated the approximate flow rate in human rete testis to each efferent ducts as  $6 \times 10^{-3} \text{ ml/h}$  with corresponding values  $a = 50 \mu\text{m}$ , frequency of the cilia beat as 20/sec and  $c = (20 \text{ beats/sec}) \times 10 \mu = 200 \mu/\text{sec}$  on the basis of experimental observations [8, 24, 25] of the flow rates in the rete testis of rat, ram, and bull. The said quantities validate the action of long wavelength and small Reynolds number theory ( $Re \ll 1$ ) in this study. Lardner and Shack [1] calculated the Non-dimensional and dimensional flow rate to respectively  $2.2 \times 10^{-2}$  and  $0.12 \times 10^{-3} \text{ ml/h}$  was evaluated by Lardner and Shack [1] from their model in the case of free pumping assuming  $\epsilon = 0.1$ ,  $\delta = 0.1$  and  $\alpha = 1$ . But, if the above said values are retained in the present study under the consideration  $n = 1$ , this model gives the non-dimensional flow rate in an axisymmetric tube as  $4.54514 \times 10^{-2}$  and consequently, the dimensional flow rate is  $0.257 \times 10^{-3} \text{ ml/h}$  (cf. Fig. 2a). This value, for an axisymmetric tube is about twice the value reported by Lardner and Shack [1] for a two-dimensional channel flow. The reason for this large difference is that they estimated flow rate initially for a channel and used it for an axisymmetric case. However,  $\epsilon$  is linearly proportional to the cilia length on the basis of the assumption and  $n$  is linked to the rheological fluid (widely known as non-Newtonian power-law fluid) in the ductus efferentes of the male reproductive tract. It has been seen from Fig. 2 that the flow rates increase significantly with an increase in  $\epsilon$ . The fact, the flow rates increase with cilia length, was also reported in [50]. Moreover, for higher values of  $\epsilon$ , rheological fluid index  $n$  remarkably affect the fluid transport for adverse pressure gradient (i.e. at pumping zone). If we consider  $n = 4/3$ ,  $\epsilon = 0.4$ ,  $\Delta P = 0$ ,  $\delta = 0.1$  and  $\alpha = 1$  then the non-dimensional flow rate and dimensional flow rate are calculated as 0.581611 and  $3.2889 \times 10^{-3} \text{ ml/h}$  respectively



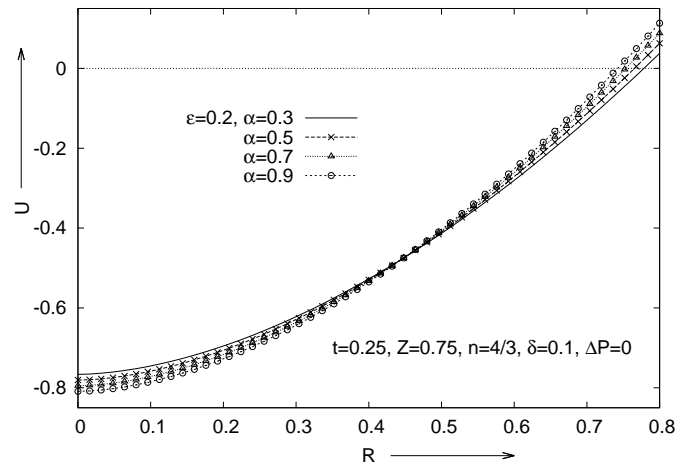
(a) Velocity profiles for a shear thinning fluid at the wave crest



(b) Velocity profiles for a shear thinning fluid at the wave trough



(c) Velocity profiles for a shear thickening fluid at the wave crest



(d) Velocity profiles for a shear thickening fluid at the wave trough

Figure 11: The diagrams exhibit the velocity profiles of the rheological fluids at the crest and the trough section for the different values of  $\alpha$ .

which is near to the estimated value  $6 \times 10^{-3} \text{ ml/h}$ . But authors have no idea about the actual length of cilia and hence the value of  $\epsilon$ , due to non-unavailability of real physiological data of the concerned variables and parameters used in the analysis. The length of cilia in ductus efferentes is measured about  $5 \mu\text{m}$  in length in the domestic fowl,  $7 \mu\text{m}$  in the guinea-fowl and quail, and  $8 \mu\text{m}$  in the turkey (*Meleagris gallopavo*).

## 5 Summary and Conclusion

Here, we have presented an analysis for the rheological fluid transport by means of a sequence of beat of cilia which are in an array and coordinated in such a way to represent the metachronal rhythm. The objective of the present study is related to the questions connecting the understanding of the fluid movement through the efferent ducts of male reproductive tract of human ([3, 21]) and the influence of cilia on ovum and sperm movement in fallopian tubes etc. However, an application of the our results for the flow rates in efferent ducts of male reproductive tract has been discussed here. On the basis of the derived analytical expressions, extensive numerical computations have been carried out. The effects of various parameters, such as  $\epsilon$ ,  $n$ ,  $\delta$ ,  $\alpha$  on pumping characteristic and velocity distribution are investigated in detail in the case of an axisymmetric tube flow.

The study reveals that for a particular set of values, say  $\epsilon = 0.1$ ,  $\delta = 1$ ,  $\alpha = 1$ ,  $n = 1$ ,  $\Delta P = 0$  (as considered in [1]) flow rate in an axisymmetric tube is about twice the value reported by Lardner and Shack [1] for a two-dimensional channel. It further reveals that the flow rate changes remarkably with  $\epsilon$  and  $n$ . When  $\epsilon$  is near about 0.4, our result for flow rate in human ductus efferentes is close to the estimated value  $6 \times 10^{-3} \text{ ml/h}$  as suggested by Lardner and Shack [1] based on the experimental observations for the flow rates in efferent ducts in other animals e.g. rat, ram, and bull.

The respectable variation between the theoretical and the measured quantities indicates that the metachronal wave of cilia cannot be responsible for the total flow rate in efferent ducts and there must be some other important factors accountable for semen movement. These factors may be (cf. Ilio and Hess [3]) (a) contraction of smooth muscle (b) invariable fluid secretion in seminiferous epithelium (c) contraction of the myoepithelial layer of seminiferous tubule as well as tunica albuginea in testis (d) the devoid space generated due to ejaculation of sperm from the lower tract and by fluid absorption (e) augmented pressure because of the design of branching and convergence of ductuli. Another important factor may be the shape of an enve-

lope of the tips of cilia beat which is different from the one considered by researchers including us. This motivates us to study the flow through ductus efferentes in the future. Consequently, for adequate understanding the mechanism involved in semen movement in ductus efferentes of male reproductive tract, further theoretical and experimental investigations are required. It may be noted that forward flow takes place at the wider portion of the tube, while backward flow occurs at narrower portion of the tube as observed earlier [30, 31, 52, 57], although forward flow is dominant for positive time-averaged flow rate.

**Acknowledgment:** *One of the authors, S. Maiti, is grateful to the University Grants Commission (UGC), New Delhi for awarding the Dr. D. S. Kothari Post Doctoral Fellowship during this investigation.*

## References

- [1] Lardner, T. J. and Shack, W. J. Cilia transport, *Bull. Math. Biol* **34**, 325-335 (1972).
- [2] Hess, R. A. Small tubules, surprising discoveries: from efferent ductules in the turkey to the discovery that estrogen receptor alpha is essential for fertility in the male, *Anim. Reprod.* **12**(1) (2015), 7-23.
- [3] Ilio, K. Y. and Hess, R. A. Structure and Function of the Ductuli Efferentes: A Review, *Microscopy Res. Tech.* **29** (1994), 432-467.
- [4] Rivera, J. A. *Cilia, Ciliated Epithelium, and Ciliary Activity*. New York: Pergamon Press (1962)
- [5] Sleight, M. A. *The Biology of Cilia and Flagella*, New York: MacMillan (1962).
- [6] Sleight, M. A. Patterns of Ciliary Beating, *In Aspects of Cell Motility*, pp. 131. Soc. Expl. Biol. Symp. X X I I . New York: Academic Press (1968).
- [7] Lucas, A . M. Ciliated Epithelium, *Special Cytology* **1**, 409-473 (1932).
- [8] Setchell, B . P . *Testicular Blood Supply, Lymphatic Drainage, and Secretion of Fluid*, The Testis, Vol. 1. (1970).
- [9] Winet, H. On the mechanism for flow in the efferent ducts, *J. Andrology* **1**(6), 304-311 (1980).



- [10] Benoit, M. J. Recherches anatomiques, cytologiques et histophysiologiques sur les voies excrétrices du testicule, chez les mammifères. *Arch. Anat, Histol. Embryol.*, 5:173-403 (1926).
- [11] Aire, T.A. and Josling, D., Ultrastructural study of the luminal surface of the ducts of the epididymis of gallinaceous birds, *Onderstepoort Journal of Veterinary Research*, 67, 191-199 (2000).
- [12] Borell, U., O. Milsson, and Westman, A. Ciliary Activity in the Rabbit Fallopian Tube During Oestrus and After Copulation, *Acta Obst. Gynee. Scand.* **36**, 22-28 (1957).
- [13] Jahn, T. L. and Bovee, E. C. Movement and Locomotion of Microorganism, *Ann. Rev. Microbiology* **19**, 21-58 (1965).
- [14] Jahn, T. L. and Bovee, E. C. *Motile Behaviour of Protozoa*, In reeseearch in proto-zoology, Vol. 1. New York: Pergamon Press, pp. 40 (1967).
- [15] Blake, J. R. A model for the microstructure in ciliated micro-organisms, *J. Fluid Mech.* **55**, 1-23 (1972).
- [16] Blake, J. R. A Spherical Envelope Approach to Ciliary Propulsion, *J. Fluid Mech.* **46**, 199-208 (1971).
- [17] Miller, C. E. An Investigation of the Movement of Newtonian Liquids Initiated and Sustained by the Oscillation of Mechanical Cilia, *Prec. 5th Cong. Appl. Mech.*, 715-720 (1966).
- [18] Miller, C. E. An Investigation of the Movement of Newtonian Liquids Initiated and Sustained by the Oscillation of Mechanical Cilia, *Aspen Emphysema Conf.*, 309-321 (1967).
- [19] Miller, C. E. Streamlines, Steak Lines and Particle Pathlines Associate with a Mechanically-induced Flow Holomorphic with the Mammalian Mucociliary System, *Biorheology* **6**, 127-135 (1969).
- [20] Barton, C. and Raynor, S. Analytical Investigation of Cilia Induced Mucous Flow, *Bull. Math. Biophysics* **29**, 419-428 (1967).
- [21] Greep, R. D., *Histology*. New York: Blakiston Division, McGraw-Kill. (1983)
- [22] Blandau, R. J. *Gamete Transport—Comparative Aspects*, In *The Mammalia Oviduct*, Hafez, E. S. and Blandau, R. J. eds. Chicago: Univ. of Chicago Press, 129-162 (1969).

- [23] Sturgis, S. H. The Effect of Ciliary Current on Sperm Progress in Excised Human Fallopian Tubes, *Trans. Amer. Soc. Study Sterility*, **3**, 31-39 (1947).
- [24] Tuck, R. R, Setchel B. P., Waites, G. M. H. and Young J. A. The Composition of Fluid Collected by Micropuncture and Catherization from the Seminiferous Tubules and Rete Testis of Rats, *Pflugers Arch.*, **318**, 225-243 (1970).
- [25] Waites, G. M. H. and Setchell, P. P. *Some Physiological Aspects of the Function of the Testis*, In *The Gonads*, K. W. McKerns, ed. New York: Appleton (1969)
- [26] Malek J., Necas, J. and Rajagopal, K. R. Global existence of solutions for fluids with pressure and shear dependent viscosities, *Appl. Math. Let.* **15**, 961-967 (2002).
- [27] Dunn, P. F. and Picologlou, B. F. Investigation of rheological properties of human semen, *Biorheology* **14**, 277-292 (1977).
- [28] Mendeluk, G., Flecha, F. L. G, Castello, P. R. and Bregni, C. Factors Involved in the Biochemical Etiology of Human Seminal Plasma Hyperviscosity, *Journal of Andrology* **21**(2), 262-267 (2000).
- [29] Xue, H. The modified Casson's equation and its application to pipe flows of shear thickening fluid, *Acta Mechanica Sinica* **21**, 243-248 (2005).
- [30] Misra, J. C. and Maiti, S. Peristaltic transport of rheological fluid: model for movement of food bolus through esophagus, *Appl. Math. Mech.* **33**(3), 15-32 (2012).
- [31] Misra, J. C. and Maiti, S. Peristaltic pumping of blood through small vessels of varying cross-section, *Trans. ASME J. App. Mech.* **22**(8), 061003 (19 pages) (2012).
- [32] Misra, J. C. and Pandey, S. K. Peristaltic flow of a multi-layered power-law fluid through a cylindrical tube, *Int. J. Engn. Sci.* **39**, 387-402 (2001).
- [33] Maiti, S. and Misra, J. C. Peristaltic Transport of a Couple Stress Fluid: Some Applications to Hemodynamics, *J. Mech. Med. Biol.* **12**(3), 1250048 (21 pages) (2012).
- [34] Liu, Y and Boling, G. Coupling model for unsteady MHD flow of generalized Maxwell fluid with radiation thermal transform, *Appl. Math. Mech.* **37**(2), 17-150 (2016).

- [35] Hayat, T., Asad, S. and Alsaedi, A. Flow of Casson fluid with nanoparticles, *Appl. Math. Mech.* **37**(4), 459-470 (2016).
- [36] Siddiqui, A. M., Ashraf, H., Walait, A. and Haroon, T. On study of horizontal thin film flow of Sisko fluid due to surface tension gradient, *Appl. Math. Mech.* **36**(7), 847-862 (2015)
- [37] Ding, Z., Jian, Y. and Yang, L. Time periodic electroosmotic flow of micropolar fluids through microparallel channel, *Appl. Math. Mech.* **36**(6), 769-786 (2016)
- [38] Srivastava, L. M and Srivastava, V. P. Peristaltic transport of a power-law fluid: Application to the ductus efferentes of the reproductive tract, *Rheol. Acta* **27**(4), 428-433 (1988).
- [39] Usha, S. and Rao, A. R. J Biomech Eng. 1997 Nov;119(4):483-8. Peristaltic transport of two-layered power-law fluids, *J. Biomech. Eng.* **119**(4), 483-488 (1988).
- [40] Rao, A. R. and Mishra, M., Peristaltic transport of a power-law fluid in a porous tube, *J. Non-Newtonian. Fluid Mech.* **121**(2-3), 163-174 (2004).
- [41] Childress, S., *Mechanics of Swimming and Flying* (Cambridge University Press, Cambridge, England, 1981.
- [42] Lauga, E and T.R. Powers. The hydrodynamics of swimming microorganisms, *Rep. Prog. Phys.* **72**, 096601 (2009)
- [43] Blake, J. R. Flow in tubules due to ciliary activity, *Bull. Math. Biol* **35**, 513-523 (1973).
- [44] Vlez-Cordero, J. R. and Lauga, E. Waving transport and propulsion in a generalized Newtonian fluid, *J Non-Newtonian Fluid Mech.*, **199**, 37-50 (2013).
- [45] Brennen, C. An oscillating-boundary-layer theory for ciliary propulsion, *J. Fluid Mech.* **65**, 799 (1974)
- [46] Lauga E. Propulsion in a viscoelastic fluid, *Phys. Fluids* **19**, 083104 (2007).
- [47] Lauga E. Life at high Deborah number. *Europhys. Lett.*, **86**:64001, (2009)
- [48] Siddiqui, A. M, Haroon, T., Rani, R. and Ansari A. R. An analysis of the flow of a power law fluid due to ciliary motion in an infinite channel, *J. Biorheol.* **24**, 56-69 (2010).

- [49] Agarwal H. and Anawaruddin. Cilia transport of bio-fluid with variable viscosity, *Indian J Pure Appl Math.* **15**(10), 1128-1139 (1984).
- [50] Blake, J. R. On the movement of mucus in the lungs, *J. Biomech.* **8**, 179 (1975)
- [51] Satir, P. Studies of Cilia; The Fixation of the Metachronal Wave, *J. Cell Biology* **18**, 345-365 (1963).
- [52] Maiti, S. and Misra, J. C. Non-Newtonian characteristics of peristaltic flow of blood in micro-vessels, *Commun. Nonlinear Sci. Numer. Simul.* **18**, 1970-1988 (2013).
- [53] Shapiro, A. H., Jaffrin, M. Y. and Weinberg, S. L. Peristaltic pumping with long wavelength at low Reynolds number, *J. Fluid Mech.* **37**, 799-825 (1969).
- [54] Moulik, S., Gopalkrishnan, K., Hinduja, I and Shahani, S. K. Presence of sperm antibodies and association with viscosity of semen, *Hum Reprod.* **4**, 290-291 (1989).
- [55] Fawcett, D. *Cilia and Flagella*, In *The Cell*, Braehet, J. and A. E. Mirsky, eds. New York: Academic Press (1961).
- [56] Bird, R.B., Stewart, W.E. and Lightfoot, E.N. *Transport Phenomena*, *John Wiley & Sons*, Singapore, 1960.
- [57] Takabatake, S. and Ayukawa, K. Numerical study of two-dimensional peristaltic flows, *J. Fluid Mech.* **122**, 439-465 (1982).